KDU Journal of Multidisciplinary Studies (KJMS)
Volume 65. Issue 2 Nov 2024
DOI: https://doi.org/10.4038/kjms.v6i2.137

KJMS 2024 VOL.6 (2): 157-171

INVESTIGATING THE MEAN TEMPERATURE OF ACCRETION DISKS AND MASS TRANSFER RATES IN CATACLYSMIC VARIABLE STARS THROUGH ORBITAL CHARACTERISTICS

Tissera PRS[1], Medagangoda NI[2], Bandara NS[1], Dharmathilaka JADM[1], and Aponsu GMLP[1]

Department of Physical Sciences and Technology, Faculty of Applied Sciences, Sabaragamuwa University of Sri Lanka[1]
Arthur C Clarke Institute for Modern Technologies, Katubedda, Moratuwa, Sri Lanka[2]

ABSTRACT

Cataclysmic variable (CV) stars, characterized by their dynamic binary systems composed of a white dwarf and a donor red dwarf star, exhibit intricate mass transfer processes crucial for understanding their evolutionary pathways. This study delved into the theoretical investigation of mass transfer processes occurring within non-magnetic CV stars analyzing their orbital characteristics. A selection of eleven CV systems, encompassing a diverse range of subcategories, were chosen for the analysis of this research. Well-established Fourier and Lomb-Scargle algorithms were utilized to identify the most effective algorithm in determining the periodicity of their light curves. The calculated orbital periods for the aforementioned CV sample were then leveraged to determine the mean temperature of their accretion disks. This determination was achieved through established techniques which used spectroscopic Balmer emission lines and Stromgren photometric observations. These techniques provide robust measurements of the physical properties of accretion disks within CVs. Finally, a strong correlation was established between mean temperature of the disk which determined through spectroscopic method and system's mass transfer rate which determined via various techniques and algorithms.

KEYWORDS: *ACCRETION DISK, CATACLYSMIC VARIABLE STARS, MASS TRANSFER RATE, ORBITAL PERIODS*

Corresponding Author: Tissera PRS, Email:ravindusadeep1@gmail.com

https://orcid.org/0009-0009-6648-6625

1. INTRODUCTION

Cataclysmic variable stars, also referred to as explosive variables, are variable stars that vary their brightness based on phenomena like flares or mass ejections of a star. Typically, CVs are binary star systems that have a white dwarf and a normal star companion (which can be a red giant). The white dwarf is referred to as the "primary" star and the normal star as the "companion" or the "secondary" star. The secondary star loses material onto the white dwarf via accretion and create an accretion disk around the primary star. CVs are mainly divided into two types, namely, Non-magnetic CVs and Magnetic CVs. The classification depends on the strength of the magnetic field of the white dwarf. Both types have several subtypes of CVs. Classical Novae, Recurrent Novae, Dwarf Novae, Novae Likes are the main subtypes of the non-magnetic CVs, while Polars and Intermediate Polars are the subtypes of magnetic CVs.

In non-magnetic CVs, the released matter from the secondary star which was under the gravitational attraction of the primary star (white dwarf), do not fall directly to the surface of the white dwarf but create an accretion disk around the primary star. This heated accretion disk, white dwarf, the hot spot of the accretion disk (and occasionally the side of the secondary star which face towards the white dwarf) are the main luminous areas that the observers could observe, and these observations can be used to derive intrinsic properties of the systems like mass transferring rates from secondary to primary, CV evolutions likewise.

Mass Transfer Rate

The mass transfer rate is the main parameter of the accretion disk temperature structure and if the accretion is assumed to be in local thermal equilibrium, temperature of the disk with radius can be stated as,

$$T(R)=(T_*)\{(R_w/R)^3[1-(R_\omega/R)^{1/2}]\}^{1/4}$$

Equation 1

Where the R_w is the radius of the white dwarf, R is the radius of the accretion disk which is correspond to the *T(R)*. T_* is defined in the [Pringle (1981)] as,

$$T_* = [3GM_\omega\dot{M}/8\pi\sigma(R_w)^3]^{1/4}$$

Equation 2

Where G, M_w, σ are universal gravitational constant, mass of the white dwarf and the Stefan-Boltzmann constant respectively.

The mean temperature of the disk can be defined as,

$$T_m=(1/A_{disk})_i\int^e T(R)\, dA$$

Equation 3

Where A_{disk} is the area of the accretion disk.

If the corresponding radiuses for the integral limits of the T_m are taken as R_i and R_e then the disk area and *dA* can be stated, $A_{disk} = \pi(R_e^2 - R_i^2)$ and $dA = 2\pi RdR$ and substituting the *T(R)* from Newton's generalization of Kepler's third law gives the T_m as,

$$T_m = \{[2(T_*) R_w^{3/4}]/[R_e^2 - R_i^2]\}\ {}_i\int^e[R- R_w^{1/2} R^{1/2}]^{1/4}\, dR$$

Equation 4

Where R_i and R_e are inner radius and the outer radius of the disk.

If we assume the mass transfer is independent from the R and the mass rate is constant throughout the accretion disk and then it would become,

$$\log \dot{M}(gs^{-1}) = 17.35 - 4 \log \xi + 4 \log (T_m/10^4) - \log (M_w/M_\odot)$$

Equation 5

Where $M_\odot$ is solar mass and

$$\xi\ (cm^{-3/4}\ 10^8) = 10^8/ (R_e^2 - R_i^2) \times {}_i\int^e[R- R_w^{1/2} R^{1/2}]^{1/4}\, dR$$

Equation 6

For the given set of R_w, R_e and R_i the ξ can be solved numerically. Echevarria (1994) stated that the ξ does not greatly depend on the R_w and R_i for larger outer radiuses the log(ξ) almost independent from the R_w

and R_i.So the log(ξ) depends on the external radius greatly. Then the ξ become,

$$\xi/10^8 = [4(R_e^{5/4} - R_i^{5/4})]/[5(R_e^2 - R_i^2)]$$

Equation 7

For the $R_e >> R_i$

$$\xi/10^8 \approx (4R_e^{-3/4})/5$$

Equation 8

The solutions for the ξ behave according to the $R_e^{-3/4}$ value for most of the R_e values. Thus, Echevarria (1994) suggests an analytical approximation to the integral with $R_e^{-3/4}$ term, multiplied by a factor which is less than unity and which accounts for deviations of ξ at small values of R_e given by,

$$\log \xi = 7.90 - (3\log R_e)/4 + \log [1 - 1.15(R_i R_w/ R_e^2)^{2/5}]$$

Equation 9

Then the mass transfer rate can be written as,

$$\log \dot{M}(gs^{-1}) = 15.74 + 4 \log (T_m/10^4) + 3 \log (R_e/10^{10}) - 4 \log [1 - 1.15(R_i R_w/ R_e^2)^{2/5}] - \log (M_w/M_\odot)$$

Equation 10

Equation 10 can be stated from the term of orbital period by using Roche lobe, orbital period relationship that holds for all the semi-detached binary and we take [Echevarria (1983)] modified to the primary star;

$$(R_L/R_\odot) = 0.2400 (M_w/M_\odot)^{1/3} P(h)^{2/3}$$

Equation 11

Where the *P(h)* is the orbital period of a system in term of hours.

For $R_w = aR_i$ and $R_e = bR_L$ where the a and b constant values substitute by using the (Hamada & Salpeter, 1961) mass radius relation for white dwarfs. We assume that the mass-radius relationship is valid for the cataclysmic variables.

From the analytical approximation of Paczynski (1985) and Anderson (1988) the relationship becomes,

$$(R_w/R_\odot) = 0.0128 (M_w/M_\odot)\times[1 - (M_w/1.458M_\odot)^{4/3}]^{0.47}$$

Equation 12

From substituting the relationship to the Equation 2.10 then it became,

$$\text{Log } \dot{M} = 16.41 + 4 \log (T_m/10^4) + 2 \log [P(h)] + 3 \log b + 4 \log \{1 - ([0.1102a^{-0.4}/ b^{0.8}][M_w/M_\odot]^{-8/15}).[1-(M_w/1.458M_\odot)^{4/3}]^{0.37}.[P(h)^{8/15}]\}$$

Equation 13

Of the last two terms which have opposite signs, with the first one dominating for a combination of very massive white dwarfs, low values of *b* and values of *an* approaching unity. Since the last term is always greater than zero it tends to balance the 3log(b) term, especially for systems with low mass white dwarfs and small values of *a*. [Echevarria (1994)] showed there that for most cases we can safely set *a* and *b* equal to unity, and have a simplified mass transfer rate relation become,

$$\text{Log } \dot{M} = 16.41 + 2 \log P(h) + 4 \log (T_m/10^4)$$

Equation 14

Determination of Mean Temperature Using Spectroscopic Method

Obtaining disc temperatures from emission line ratios could be an unreliable process, since the lines could be formed only within the external parts of the disc, where they are the main coolant. During this case we will observe a kinetic temperature of the external parts which is constant. Accordingly, if the lines are formed during a photo-ionized region above the disc, the line temperatures are probably going to be fixed at a temperature close to 10000K. There are, however, more samples of cataclysmic variables which Balmer lines present very broad wings indicating large velocities which may only be explained if they are formed at the inner parts of the disc. Moreover, the road ratios in many of those objects have values which

follow very simple LTE calculations for a series of uniform layers of hydrogen at high densities. It is also important to understand what range of values we should always expect Echevarria (1994).

Figure 04 in Echevarria (1994) shows the mean temperature as a function of external disc radius for various mass transfer rates. These are derived using the numerical integrations of ξ, with log Rw = 8.90, log Ri = 8.95 and assuming log Mw = 0. just for very large mass transfer rates the mean temperature rises above 30000K. For log ($\dot{M}$) < 16 it falls below 10000K for all values of Re. the rationale for this behaviour is just that the lower temperatures within the disc dominate because they're produced at much larger areas than the inner accretion rings.

Comparison with the line ratios calculated by Drake and Ulrich (1980) for a high-density uniform slab of hydrogen indicates that the Balmer decrement of cataclysmic variables is a function of the mean temperature in the emitting region of the accretion disk of the primary. The accretion discs are not a slab of uniformly distributed density at the same temperature, but we may think of them as a series of uniform density rings at several temperatures. This collection of rings will show the mean temperature value, and the mean temperature can be used to find the mass transfer rate.

The Doppler line profile can be given by Balmer line profiling using the ratio between H_γ/H_β and H_δ/H_β. The relevant equations as follows Drake and Ulrich (1980).

$$H_\gamma/H_\beta = 1.57 \{[\exp(29599/T_m) - 1]/[\exp(33153/T_m) - 1]\}$$

Equation 15

And,

$$H_\delta/H_\beta = 1.97 \{[\exp(29599/T_m) - 1]/[\exp(35085/T_m) - 1]\}$$

Equation 16

The line ratios must be corrected for the interstellar absorption, and it can be calculated by the following,

$$\log [I(\lambda)/I(H_\beta)] = \log [F(\lambda)/F(H_\beta)] + C(H_\beta)f(\lambda)$$

Equation 17

Where the F(λ), C(H_β), f(λ)are observed flux, logarithmic reddening correction at H_β and reddening function normalized at H_β which derived by normal extinction law (Whitfold, 1958).

Determination of Mean Temperature Using Strömgren Photometry

Another method to determine the mean temperature of a CV system is to use broad band photometry of the disk continuum. First step is to derive a relationship between mean temperature and Strömgren b-y index. Then the relationship can be used to find the mass transfer rate according to the Strömgren b-y index.

Echevarria (1994) suggested a logarithmic relationship between b-y index and the mean temperature as follows.

$$\text{Log } (T_m/10^4) = A + B \log (b\text{-}y)$$

Equation 18

Figure 09 in Echevarria (1994) gives the values for the A and B for both blackbody approximations and the main sequence star approximations according to Crawford (1975), Crawford (1979) and Johnson (1966). For blackbody approximation A = - 0.303 and B = - 0.187 (Hayes & Lathem, 1975). For main sequence star's approximation, A = - 0.316 and B = - 0.236 (Crawford, 1975; Crawford, 1979; Johnson, 1966).

Then the Equation 18 is changed as follows for both approximations accordingly.

For blackbody approximation,

$$\text{Log } (T_m/10^4) = - 0.303 - 0.187 \log (b - y)$$

Equation 19

For main sequence star approximation,

$$\text{Log } (T_m/10^4) = - 0.316 – 0.236 \log (b – y)$$

Equation 20

So according to the relationship between mean temperature and Strömgren b-y indices, we can derive the new relationship among orbital period, Strömgren b-y index and mass transfer rate for both approximations. For blackbody approximations;

$$\text{Log } \dot{M} = 15.20 + 2 \log P(h) – 0.75 \log (b – y)$$

Equation 21

And for main sequence star approximations;

$$\text{Log } \dot{M} = 15.14 + 2 \log P(h) – 0.94 \log (b – y)$$

Equation 22

We will use the black body approximation to derive the mass transfer rate because the main sequence star can generate slightly higher values than actual values Echevarria (1994).

Research Gap

While significant studies have been conducted on cataclysmic variable stars (CVs), the understanding of how orbital characteristics, the mean temperature of accretion disks, and mass transfer rates are interconnected is still insufficient. Most existing research either focuses on one aspect, such as temperature distribution of accretion disk or mass transfer rates, without connecting these parameters to each other.

Objective

This research will investigate observational data from multiple CVs and their impact on the mass transfer rate and mean temperature of the accretion disks.

2. METHODOLOGY

Cataclysmic Variable star systems were chosen in a variety of types for analysis.

Further, their respective properties were also analyzed under the scope of the present research.

Table 01: Selected cataclysmic variable star systems

Name of the CV	Type of the CV
GK Per	UG/NA
EM Cyg	UGZ
AH Her	UGZ
U Gem	UGSS
EX Hya	UG
RU Peg	UGSS
SS Cyg	UGSS
SS Aur	UGSS
TW Vir	UGSS
YZ Cnc	UGSU

UG, NA, UGZ, UGSS, UGSU are U Geminorum-type variables (often called as dwarf novae), fast novae, Z Camelopardalis-type variables, SS Cygni-type variables and SU Ursae Majoris-type variables respectively.

Light Curves of the CV systems

As a basic source for the variable star observations retrieval and further details of variable stars the AAVSO database (American Association of Variable Stars Observers) was used (https://www.aavso.org/). The raw observation data from AAVSO including observation dates (in Julian dates), magnitude, uncertainty of the observation, observation bands, observer Code were downloaded from the AAVSO as a tab delimited text file for further analysis. The data obtained by the AAVSO required several filtering processes to achieve the required data format for the

further analysis. The raw data was contained data under following columns. JD(Julian dates), Magnitude, Uncertainty, HQuncertainty, Band, Observer Code, Comment Code(s), Comp Star 1, Comp Star 2, Charts, Comments, Transfomed, Airmass, Validation Flag, Cmag, Kmag, HJD, Star Name, Observer Affiliation, Measurement Method, Grouping Method, ADS Reference, Digitizer, Credit. From these columns as previously stated the time (Julian dates), observe magnitudes and the error of the magnitude data were filtered for a single observer. The filtering process for the single observer is important to avoid generating of incorrect light curves by overlapping observations over time for a single system.

As the next and more specific database by observations SuperWASP database was used to access the raw observations (https://www.superwasp.org/).

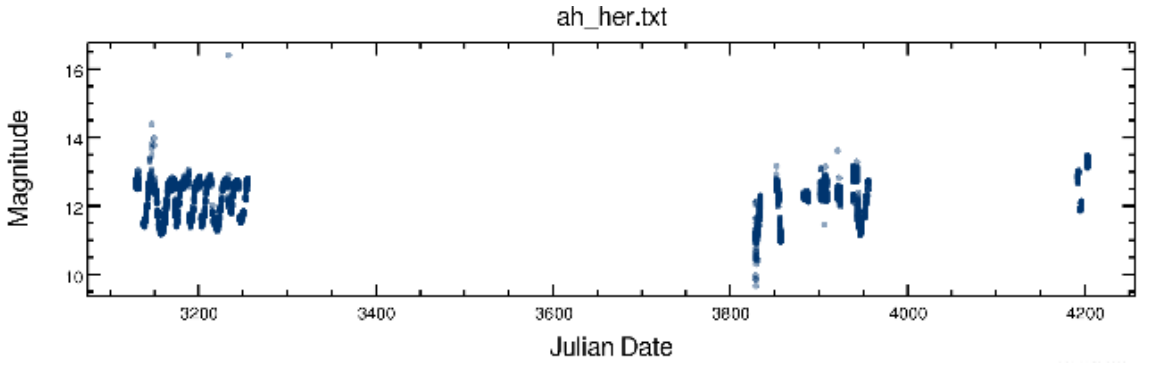

Figure 01: Light curve data of AH Her CV system

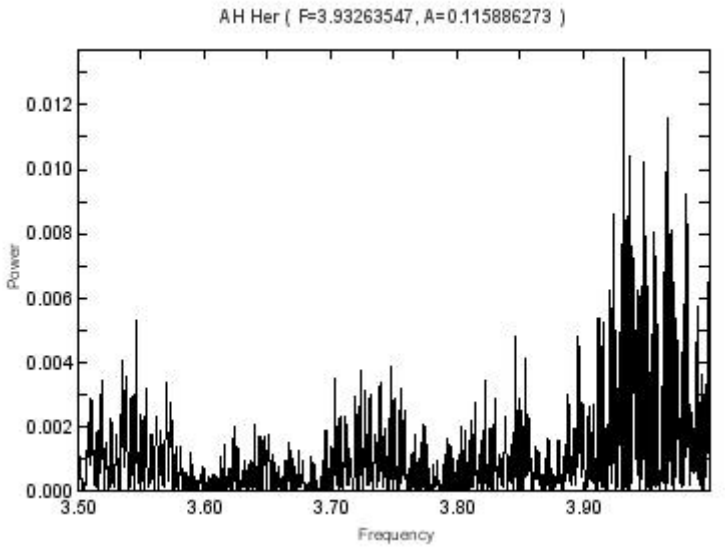

Figure 02: Power Spectrum of AH Her for Fourier algorithm using Period04

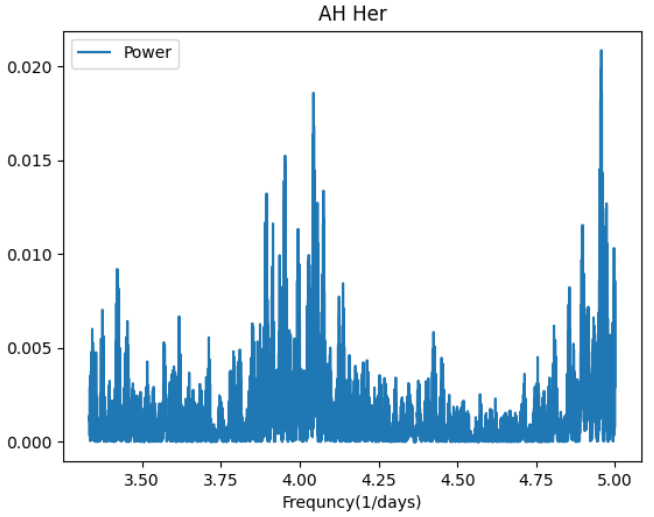

Figure 03: Power Spectrum of AH Her for Lomb-Scargle algorithm by Vartool

The data downloaded from the SuperWASP database did not require filtering because the downloadable .CSV file only contained time (Julian dates), observed magnitudes and the error of the magnitude by the WASP telescopes.

For the analysis of the light curve Period04, Vartools and NASA exoplanet periodogram tools were used, depending on the spread of the light curve. To obtain the power spectrum of the light curves, both Fourier and Lomb-Scargle analysis algorithms were used.

Stromgren photometric observations

Table 02: Stromgren photometric observations of the CV systems, (Echevarria (1994))

Name of the CV	b	y	(b-y)
GK Per	13.34	12.77	0.57
EM Cyg	13.45	13.16	0.29
AH Her	12.67	12.55	0.12
AH Her	12.92	12.77	0.15
U Gem	14.43	14.19	0.24
U Gem	14.91	14.59	0.32
U Gem	14.13	13.84	0.29
EX Hya	14.12	13.95	0.17
RU Peg	13.34	12.81	0.53
SS Cyg	12.23	11.7	0.53
SS Aur	15.12	14.97	0.15
SS Aur	11.01	10.99	0.02
SS Aur	11.13	11.11	0.02
TW Vir	13.16	13.12	0.04
YZ Cnc	13.6	13.47	0.13
YZ Cnc	15.38	15.17	0.21
YZ Cnc	12.14	12.13	0.01
IR Gem	12.8	12.79	0.01

Spectroscopic observations

Table 03: Observations of Balmer emission lines H_β,H_δ,H_γ and $C_{H\beta}$, (Echevarria (1994))

Name	EW(H_β)	FHγ	FH$_\delta$	CH$_\beta$
GK Per	11	0.85	0.57	0.32
EM Cyg	11	0.96	-	0.07
	3	1.15	-	0.07
AH Her	24	0.9	-	0.04

	26	0.84	0.82	0.04
U Gem	15	0.85	0.81	0.04
EX Hya	74	0.65	-	0.05
RU Peg	4	1.02	0.45	0.08
	5	0.98	0.66	0.08
	16	1.19	1.49	0.08
	28	0.72	-	0.08
SS Cyg	40	0.81	0.74	0.06
	74	0.8	-	0.06
	70	0.76	0.66	0.06
	67	0.76	0.57	0.06
	30	1.08	1.02	0.06
	32	0.98	0.49	0.06
	25	1.17	1.35	0.06
SS Aur	58	0.72	0.53	0.15
	76	0.89	-	0.15
	95	0.84	0.73	0.15
	106	0.82	0.67	0.15
	122	0.85	0.58	0.15
TW Vir	78	0.92	0.75	0.2
	14	0.89	0.73	0.2
	70	0.73	0.6	0.2
	96	0.85	0.78	0.2
	73	1.05	0.99	0.2
YZ Cnc	80	0.89	0.76	0.13
	131	0.83	0.71	0.13
	42	1.01	0.97	0.13
	92	0.77	-	0.13
IR Gem	116	0.77	0.63	0.11
	81	1.08	0.87	0.11

EW = Equalent width of H_β line and the observed Balmer line widths are represented as the ratio with the H_β line. $C_{H\beta}$ = Logarithmic reddening correction at H_β

3. RESULTS AND DISCUSSION

Mean Temperature of CV systems by Photometric method

Mean temperatures by photometric method were calculated using the Equation 18 and the photometric values from Table 02.

Table 04: Mean Temperatures by Photometric method

Name	(b-y)	Tm(K)
GK Per	0.57	5529.06
EM Cyg	0.29	6273.81
AH Her	0.12	7399.34
AH Her	0.15	7096.93
U Gem	0.24	6499.81
U Gem	0.32	6159.38
U Gem	0.29	6273.81
EX Hya	0.17	6932.76
RU Peg	0.53	5604.80
SS Cyg	0.53	5604.80
SS Aur	0.15	7096.94
SS Aur	0.02	10344.45
SS Aur	0.02	10344.45
TW Vir	0.04	9086.88
YZ Cnc	0.13	7289.41
YZ Cnc	0.21	6664.15
YZ Cnc	0.01	11776.06
IR Gem	0.01	11776.06

Mean Temperature of CV systems by Photometric method

Using the Equations 15,16,17 and the values from the table 03 the mean temperature of systems were calculated.

Table 05: Mean temperatures by spectroscopic emission line widths

Name	FH_γ	FH_δ	CH_β	Tm(K)	
				H_γ	H_δ
GK Per	0.85	0.57	0.32	7000	5000
EM Cyg	0.96	-	0.07	14500	-
	1.15	-	0.07	7700	-
AH Her	0.9	-	0.04	6600	-
	0.84	0.82	0.04	5800	6500
U Gem	0.85	0.81	0.04	5900	6400
EX Hya	0.65	-	0.05	4100	-
RU Peg	1.02	0.45	0.08	9100	3850
	0.98	0.66	0.08	8000	5200
	1.19	1.49	0.08	16300	43000
	0.72	-	0.08	4700	-
SS Cyg	0.81	0.74	0.06	5600	5800
	0.8	-	0.06	5500	-
	0.76	0.66	0.06	5000	5150
	0.76	0.57	0.06	5000	4550
	1.08	1.02	0.06	10500	9000
	0.98	0.49	0.06	8000	4000
	1.17	1.35	0.06	14500	19500
SS Aur	0.72	0.53	0.15	4800	4400
	0.89	-	0.15	6800	-
	0.84	0.73	0.15	6200	5950
	0.82	0.67	0.15	5900	5450
	0.85	0.58	0.15	6300	4750
TW Vir	0.92	0.75	0.2	7600	6300
	0.89	0.73	0.2	7200	6100
	0.73	0.6	0.2	5100	5000
	0.85	0.78	0.2	6400	6700
	1.05	0.99	0.2	11000	9600
YZ Cnc	0.89	0.76	0.13	6800	6200
	0.83	0.71	0.13	5900	5700
	1.01	0.97	0.13	9100	8700
	0.77	-	0.13	5300	-
IR Gem	0.77	0.63	0.11	5300	5000
	1.08	0.87	0.11	11200	7300

Light Curve Analysis using Fourier Algorithm

Table 06: Highest peak values of Power spectrum using Fourier algorithm

Name	Frequency (1/Days)	Orbital period (Days)
GK Per	0.496279762	2.014992503
EM Cyg	3.04363308	0.328554715
AH Her	3.9326354	0.258116
U Gem	5.997668271	0.166731462
SS Cyg	3.41830001	0.292543076
TW Vir	5.002102819	0.199915923
YZ Cnc	11.76594041	0.084991082
IR Gem	14.7433678	0.067827108

From all the CV systems EX Hya, RU Peg and SS Aur didn't provide reliable power spectrums and more deviated orbital periods from the actual values for the Fourier analyze. The Fourier technique in the light curve analysis gives most reliable answers to the light curves which are the shapes of sine or cosine waves functions and continuous spectrums with minimum time gaps between observations. But for the light curves in Figure 01 for EX Hya, RU Peg and SS Aur have much larger observation gaps and less sine or

cosine shapes. For the other systems, it seems that there are no sine or cosine shapes in their light curves during the whole observation period. However, when analyzed over a shorter time span, the light curves partially show sine or cosine shapes with partially continuous observation scattering.

Light Curve Analysis using Lomb-Scargle Algorithm

Table 06: Highest peak values of Power spectrum using Lomb-Scargle algorithm

Name	Orbital period (days)
GK Per	2.01052904
EM Cyg	0.31936315
AH Her	0.24969318
U Gem	0.1687962
SS Cyg	0.2678389
TW Vir	0.19730737
YZ Cnc	0.08337633
IR Gem	0.07149026
SS Aur	0.19806165
EX Hya	0.05135202
RU Peg	0.37722567

Mass Transfer Rates Using Fourier Algorithm Results and Photometric Temperature Calculations

EM Cyg, RU Peg, and SS Aur are not considered in the calculations of the mass transfer rate in Table 07 because these systems did not provide reliable values for Fourier analysis.

Table 07: Mass transfer rates (M.T.R) for Fourier and photometric data

Name	log P (hrs)	photometry Tm (K)	M.T.R (Kgs^{-1})
GK Per	1.6844	5529.0612	5.6179×10^{15}
EM Cyg	0.8968	6273.8130	2.4760×10^{14}
AH Her	0.7855	7399.3421	2.8696×10^{14}
AH Her	0.7855	7096.9367	2.4285×10^{14}
U Gem	0.6022	6499.8075	7.3461×10^{13}
U Gem	0.6022	6159.3793	5.9238×10^{13}
U Gem	0.6022	6273.8130	6.3765×10^{13}
SS Cyg	0.8464	5604.8037	1.2503×10^{14}
TW Vir	0.6810	9086.8797	4.0343×10^{14}
YZ Cnc	0.3095	7289.4136	3.0195×10^{13}
YZ Cnc	0.3095	6664.1535	2.1093×10^{13}
YZ Cnc	0.3095	11776.0597	2.0566×10^{14}
IR Gem	0.2116	11776.0597	1.3098×10^{14}

Mass Transfer Rates Using Fourier Algorithm Results and H_γ Emission Line Temperature Calculations

Table 08: Mass transfer rates for Fourier and spectroscopic Hγ emission line data

Name	Log P (hrs)	Tm by H_γ (K)	M.T.R (Kgs^{-1})
GK Per	1.6844	7000	1.4433×10^{16}
EM Cyg	0.8968	14500	7.0650×10^{15}
EM Cyg	0.8968	7700	5.6183×10^{14}
AH Her	0.7855	6600	1.8165×10^{14}
AH Her	0.7855	5800	1.0834×10^{14}
U Gem	0.6022	5900	4.9873×10^{13}
SS Cyg	0.8464	5600	1.2461×10^{14}
SS Cyg	0.8464	5500	-
SS Cyg	0.8464	5000	7.9192×10^{13}
SS Cyg	0.8464	5000	7.9192×10^{13}
SS Cyg	0.8464	10500	1.5401×10^{15}
SS Cyg	0.8464	8000	5.1899×10^{14}
SS Cyg	0.8464	14500	5.6011×10^{15}

TW Vir	0.6810	7600	1.9741×10^{14}
TW Vir	0.6810	7200	1.5902×10^{14}
TW Vir	0.6810	5100	4.0031×10^{13}
TW Vir	0.6810	6400	9.9274×10^{13}
TW Vir	0.6810	11000	8.6634×10^{14}
YZ Cnc	0.3095	6800	2.2867×10^{13}
YZ Cnc	0.3095	5900	1.2959×10^{13}
YZ Cnc	0.3095	9100	7.3339×10^{13}
YZ Cnc	0.3095	5300	8.4386×10^{12}
IR Gem	0.2116	5300	5.3744×10^{12}
IR Gem	0.2116	11200	1.0718×10^{14}

Mass Transfer Rates Using Fourier Algorithm Results and H_δ Emission Line Temperature Calculations

Table 09: Mass transfer rates for Fourier and spectroscopic H_δ emission line data

Name	Log P (hrs)	Tm by H_δ (K)	M.T.R (Kgs^{-1})
GK Per	1.6844	5000	3.7571×10^{15}
EM Cyg	0.8968	-	-
AH Her	0.7855	6500	1.7089×10^{14}
U Gem	0.6022	6400	6.9052×10^{13}
SS Cyg	0.8464	5800	1.4339×10^{14}
SS Cyg	0.8464	5150	8.9132×10^{13}
SS Cyg	0.8464	4550	5.4306×10^{13}
SS Cyg	0.8464	9000	8.3133×10^{14}
SS Cyg	0.8464	4000	3.2437×10^{13}
SS Cyg	0.8464	19500	1.8321×10^{16}
TW Vir	0.6810	6300	9.3214×10^{13}
TW Vir	0.6810	6100	8.1929×10^{13}
TW Vir	0.6810	5000	3.6983×10^{13}
TW Vir	0.6810	6700	1.1924×10^{14}
TW Vir	0.6810	9600	5.0258×10^{14}
YZ Cnc	0.3095	6200	1.5803×10^{13}
YZ Cnc	0.3095	5700	1.1289×10^{13}
YZ Cnc	0.3095	8700	6.1270×10^{13}
IR Gem	0.2116	5000	4.2571×10^{12}
IR Gem	0.2116	7300	1.9343×10^{13}

Mass Transfer Rates Using Lomb-Scargle Algorithm Results and Photometric Temperature Calculations

Table 10: Mass transfer rates for Lomb-Scargle and photometric data

Name	log P (hrs)	photometry Tm (K)	M.T.R (Kgs^{-1})
GK Per	1.6835	5529.0612	5.5931×10^{15}
EM Cyg	0.8844	6273.8130	2.3395×10^{14}
AH Her	0.7776	7399.3421	2.7670×10^{14}
AH Her	0.7776	7096.9367	2.3416×10^{14}
U Gem	0.6075	6499.8075	7.5292×10^{13}
U Gem	0.6075	6159.3793	6.0715×10^{13}
U Gem	0.6075	6273.8130	6.5354×10^{13}
EX Hya	0.0907	6932.7581	9.0191×10^{12}
RU Peg	0.9568	5604.8037	2.0791×10^{14}
SS Cyg	0.8080	5604.8037	1.0481×10^{14}
SS Aur	0.6770	7096.9367	1.4734×10^{14}
SS Aur	0.6770	10344.4496	6.6505×10^{14}
SS Aur	0.6770	10344.4496	6.6505×10^{14}
TW Vir	0.6753	9086.8797	3.9298×10^{14}
YZ Cnc	0.3012	7289.4136	2.9059×10^{13}
YZ Cnc	0.3012	6664.1535	2.0300×10^{13}
YZ Cnc	0.3012	11776.0597	1.9793×10^{14}

IR Gem	0.2344	11776.0597	1.4552×10^{14}

Mass Transfer Rates Using Lomb-Scargle Algorithm Results and H_γ Emission Line Temperature Calculations

Table 11: Mass transfer rates for Lomb-Scargle and spectroscopic Hγ emission line data

Name	Log P (hrs)	Tm by H_γ (K)	M.T.R (Kgs^{-1})
GK Per	1.6835	7000	1.4369×10^{16}
EM Cyg	0.8844	14500	6.6752×10^{15}
EM Cyg	0.8844	7700	5.3083×10^{14}
AH Her	0.7776	6600	1.7515×10^{14}
AH Her	0.7776	5800	1.0446×10^{14}
U Gem	0.6075	5900	5.1116×10^{13}
EX Hya	0.0907	4100	1.1033×10^{12}
RU Peg	0.0907	9100	2.6773×10^{13}
RU Peg	0.0907	8000	1.5992×10^{13}
RU Peg	0.0907	16300	2.7561×10^{14}
RU Peg	0.0907	4700	1.9052×10^{12}
SS Cyg	0.8080	5600	1.0445×10^{14}
SS Cyg	0.8080	5500	9.7190×10^{13}
SS Cyg	0.8080	5000	6.6382×10^{13}
SS Cyg	0.8080	5000	6.6382×10^{13}
SS Cyg	0.8080	10500	1.2910×10^{15}
SS Cyg	0.8080	8000	4.3504×10^{14}
SS Cyg	0.8080	14500	4.6951×10^{15}
SS Aur	0.6770	4800	3.0831×10^{13}
SS Aur	0.6770	6800	1.2418×10^{14}
SS Aur	0.6770	6200	8.5820×10^{13}
SS Aur	0.6770	5900	7.0377×10^{13}
SS Aur	0.6770	6300	9.1493×10^{13}
TW Vir	0.6753	7600	1.9229×10^{14}
TW Vir	0.6753	7200	1.5490×10^{14}
TW Vir	0.6753	5100	3.8993×10^{13}
TW Vir	0.6753	6400	9.6701×10^{13}
TW Vir	0.6753	11000	8.4388×10^{14}
YZ Cnc	0.3012	6800	2.2006×10^{13}
YZ Cnc	0.3012	5900	1.2471×10^{13}
YZ Cnc	0.3012	9100	7.0579×10^{13}
YZ Cnc	0.3012	5300	8.1210×10^{12}
IR Gem	0.2344	5300	5.9706×10^{12}
IR Gem	0.2344	11200	1.1907×10^{14}

Mass Transfer Rates Using Lomb-Scargle Algorithm Results and H_δ Emission Line Temperature Calculations

Table 12: Mass transfer rates for Lomb-Scargle and spectroscopic Hδ emission line data

Name	Log P (hrs)	Tm by H_δ (K)	M.T.R (Kgs^{-1})
GK Per	1.6835	5000	3.7404×10^{15}
EM Cyg	0.8844	-	-
AH Her	0.7776	6500	1.6477×10^{14}
U Gem	0.6075	6400	7.0773×10^{13}
EX Hya	0.0907	-	-
RU Peg	0.0907	3850	8.5779×10^{11}
RU Peg	0.0907	5200	2.8546×10^{12}
RU Peg	0.0907	43000	1.3348×10^{16}
SS Cyg	0.8080	5800	1.2019×10^{14}
SS Cyg	0.8080	5150	7.4713×10^{13}
SS Cyg	0.8080	4550	4.5521×10^{13}
SS Cyg	0.8080	9000	6.9685×10^{14}
SS Cyg	0.8080	4000	2.7190×10^{13}

SS Cyg	0.8080	19500	1.5357×10^{16}
SS Aur	0.6770	4400	2.1769×10^{13}
SS Aur	0.6770	5950	7.2793×10^{13}
SS Aur	0.6770	5450	5.1240×10^{13}
SS Aur	0.6770	4750	2.9566×10^{13}
TW Vir	0.6753	6300	9.0797×10^{13}
TW Vir	0.6753	6100	7.9805×10^{13}
TW Vir	0.6753	5000	3.6024×10^{13}
TW Vir	0.6753	6700	1.1615×10^{14}
TW Vir	0.6753	9600	4.8955×10^{14}
YZ Cnc	0.3012	6200	1.5208×10^{13}
YZ Cnc	0.3012	5700	1.0864×10^{13}
YZ Cnc	0.3012	8700	5.8964×10^{13}
IR Gem	0.2344	5000	4.7293×10^{12}
IR Gem	0.2344	7300	2.1489×10^{13}

Correlation Between Mass Transfer Rate and Mean Temperature of Fourier Data with Photometric and Spectroscopic Data

Table 13: Correlations between Log (Tm/10E4) and Log (M.T.R)

Dependent Variable	Independent Variable	Correlation Coefficient	P-Value
LS_Ph_log (M.T.R)	LS_Ph_log ($Tm/10^4$)	0.159	0.530
LS_H_γ_log (M.T.R)	LS_H_γ_Log ($Tm/10^4$)	0.667	0.000
LS_H_δ_log (MTR)	LS_H_δ_log ($Tm/10^4$)	0.748	0.000
F_Ph_log (M.T.R)	F_Ph_log ($Tm/10^4$)	-0.044	0.887
F_H_γ_log (M.T.R)	F_H_γ_log ($Tm/10^4$)	0.694	0.000
F_H_δ_log (M.T.R)	F_H_δ_log ($Tm/10^4$)	0.633	0.004

LS_Ph_, LS_H_γ_, LS_H_δ_, F_Ph_, F_H_γ_ and F_H_δ_ are Lomb-Scargle data and Photometric data, Lomb-Scargle data and H_γ/H_β data, Lomb-Scargle data and H_δ/H_β data, Fourier data and photometric data, Fourier data and H_γ/H_β data, Fourier data and H_δ/H_β data respectively.

The table of correlations between the *Log(M.T.R)* and *Log(Tm/10⁴)* which were calculated using photometric and spectroscopic shows that the photometric data gives no correlations in the photometric mean temperature calculations. Although the photometric data gives correlations coefficient values the P-values for both photometric data are greater than 0.05. If there should be any correlation between independent and dependent variables the P-value must be less than 0.05. But in reality, the mean temperature of the accretion disk depends on the mass transfer rate. The reason for the formation of the accretion disk is the beginning of the mass transferring process from secondary to the primary of a CV. So, the mean temperature and the mass transfer rate should have perfect correlation with each other. It is proven by both H_γ/H_β and H_δ/H_β spectroscopic mean temperature calculations in the table 08, 09, 11, 12 and table 13. The reason for the no correlation of photometric data is the low number of observations in the Strömgren photometry. Due to that reason the normalization process for the obtaining correlation is difficult for the Strömgren photometry.

4. CONCLUSION

Although the correlation coefficient detected no correlation state between mean temperature which obtained by the Strömgren photometric, the spectroscopic analyze clearly states there are strong correlation between the variables. We suggest using a large data sample for the Strömgren photometric technique in the future works as it gives more accurate correlations between the variables.

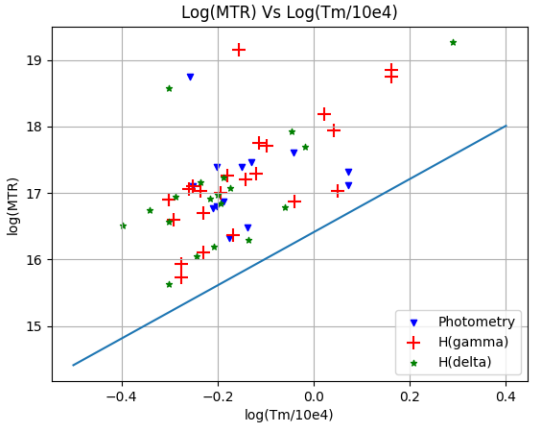

Figure 04: Log (M.T.R) Vs Log (Tm/10^4) graph for Fourier data with photometric and spectroscopic results. Solid line represents the Equation 14 for P(h) = 1hr.

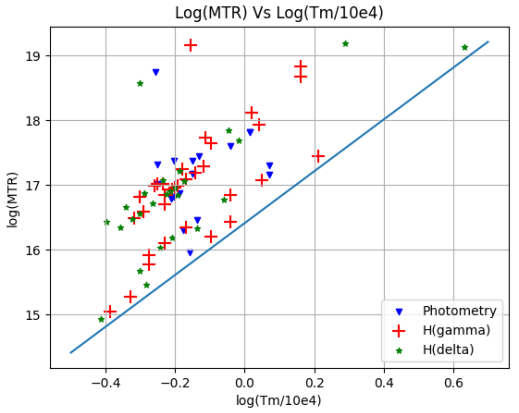

Figure 05: Log (M.T.R) Vs Log (Tm/10^4) graph for Lomb-Scargle data with photometric and spectroscopic results. Solid line represents the Equation 14 for P(h) = 1hr.

Since the emission lines or photometric observations observed in a CV are limited to several points of the model, the observations are highly dependent on the inclination angle between the CV and the observer. Also, for future interpretations, we encourage to consider a method which uses Doppler radial velocity and the inclination angle to interpret the results for mass transfer rates.

5. ACKNOWLEDGEMENT

I would like to express my gratitude to Mr. N.I. Medagangoda (senior research scientist, Arthur C Clarke Institute of Modern Technologies, Moratuwa) for the immense support and encouragement which he gave me to complete this investigation. Addition to that I extend my gratitude to Dr.N.S. Bandara, Ms. J.A.D.M. Dharmathilaka, Prof.G.M.L.P. Aponsu (Department of Physical Sciences and Technology, Faculty of Applied Sciences, Sabaragamuwa University of Sri Lanka), who were gave me the guidance to completing this research successfully.

6. REFERENCES

Anderson, N., (1988). Models of U Geminorum and Z Chamaeleontis based on disk radius variations.

Astrophysical J., Part 1: . 325, Feb. 1988, pp. 266-281. ISSN 0004-637X

Crawford, D.L., (1975). Empirical calibration of the ubvy, beta systems. I. The F-type stars. *Astronomical J.*:80, pp. 955-971, 80.

Crawford, D.L., 1979. Empirical Calibrations of the UVBY, Beta Systems-Part Three-the A-Type Stars. *Astronomical J:* 84, p. 1858, 1979.

Drake, S.A. and Ulrich, R.K., (1980). The emission-line spectrum from a slab of hydrogen at moderate to high densities. *Astrophysical J. Supplement Series:*42, pp.351-383, Feb 1980.

Echevarría, J., (1983). Are the secondary stars in cataclysmic variables main sequence stars. *Revista Mexicana de Astronomia y Astrofisica:* 8(2), p. 109, 1983.

Echevarría, J., (1994). On the mass transfer-orbital period relation in cataclysmic variables. *Revista Mexicana de Astronomia y Astrofisica*, 28(2), p. 125-137.

Hamada, T. and Salpeter, E.E., (1961). Models for Zero-Temperature Stars. *Astrophysical J.*:134, p. 683.

Hayes, D.S. and Latham, D.W., (1975). A rediscussion of the atmospheric extinction and the

absolute spectral-energy distribution of VEGA. *Astrophysical J.:*197, pp.593-601, May 1975.

Johnson, H.L., (1966). Astronomical measurements in the infrared. *Annual Rev. of Astronomy and Astrophysics*, 4(1), pp.193-206.

Paczynski, B., (1985). Evolution of cataclysmic binaries. In Cataclysmic Variables and Low-Mass X-Ray Binaries: *Pros. of the 7th North American Workshop* held in Campbridge, Massachusetts, USA, ,pp. 1-14, Jan 1983, Springer,Netherlands.

Pringle, J.E., (1981). Accretion discs in astrophysics. *Annual Rev. of Astronomy and Astrophysics:*19.(A82-11551 02-90), Palo Alto, CA, p. 137-162., 1981.

Whitford, A.E., (1958). *The law of interstellar reddening. Astronomical J.:*63, p. 201-207,1958.